2.4 Accelerator Mass Spectroscopy with Heavy Ions

At the Munich accelerator laboratory, different methods of accelerator mass spectrometry (ams) were developed and are used in the fields of applied physics, of interdisciplinary research and of fundamental aspects of physics. The methods are

a) complete stripping of postaccelerated ions, magnetic analysis and detection in a Bragg ionization chamber. This method is used for the radioisotopes ^{26}Al (716,000 y), ^{36}Cl (300,000 y), ^{41}Ca (103,000 y), ^{53}Mn (3,700,000 y) and ^{59}Ni (95,000 y).

b) Detection of ions in the gas-filled Q3D magnet spectrometer by applying the Wien velocity filter and a time-of-flight line. Up to now, we use this method for the identification of ^{59}Ni and ^{90}Sr.

c) Detection of ions in an energy loss / residual energy detector by applying the Wien velocity filter and eventually a time-of-flight line. The detector is either a combination of ΔE ionization chamber and silicon residual energy detector or is a Bragg ionization chamber. This installation has been applied for th radio isotopes ^{26}Al, ^{55}Fe and ^{129}I.

In 1992, the investigated problems were from the fields of cosmic radiation, cosmogenic radioisotopes, dosimetry, medicine and of fundamental aspects of physics.

2.4.1 Global fall-out of cosmogenic ^{36}Cl

A. Blinov [a], D. Huggle, E. Joranger [c], M. Kaba [b], G. Korschinek, S. Massonet, E. Nolte, W. Rühm, Ch. Scheffel, L. Zerle,
[a] Technical University of St. Petersburg
[b] National University of Ivory Coast, Abidjan (Ivory Coast)
[c] Norsk Institutt for Luftfroskning, NILU (Norway)

In order to determine the global fall-out rate and distribution of cosmogenic ^{36}Cl two activities have been started : a) at many meteorological stations worldwide, rainwater samples were and are collected over a time period of one year. ^{36}Cl/Cl ratios of these samples were measured and the ^{36}Cl fall-out rates were determined. b) The relevant cross sections for the production of cosmogenic ^{36}Cl in the atmosphere were and have to be measured in order to calculate the production rate of cosmogenic ^{36}Cl.

In the atmosphere, ^{36}Cl is mainly produced by spallation and nuclear compound reactions of the cosmic radiation with ^{40}Ar. At energies above 300 MeV, spallation reactions ^{40}Ar(X,Xp3n)^{36}Cl are dominant (X = p,n), at energies around 60 MeV the compound reactions ^{40}Ar(X,Xp3n) are expected to contribute and at energies around 30 MeV the compound reaction ^{40}Ar(p,αn) should take place. Other reactions as ^{36}Ar(p,n)^{36}Cl and ^{35}Cl(n,γ)^{36}Cl are estimated to give much smaller yields.

The stratospherically produced ^{36}Cl remains with a mean residence time of two years in this layer before it is exchanged mainly at mid latitudes to the troposphere from where it reaches within days together with the tropospherically produced ^{36}Cl the surface of the earth.

Fig. 1 shows the measured results of the ^{36}Cl fall-out rates in dependence of the geological latitude for the stations Ny Ålesund, Spitsbergen (77° latitude), Averbygd (68°), Tus Tervatn (64°), Karvatn (62°), Nausta (60°), Birkenes (58°, all Norway), Risø (56°, Denmark), St. Petersburg (60°), Moscow (56°), Lake Baikal (53°, all Russia), Munich (48°), Shanghai (31°, China), Ferkesse-Dougou (8°)

and Abidjan (5°, both Ivory Coast). All samples except the Russian ones give the results integrated over one year. The collection times for the Russian samples are : St. Petersburg three months, Moscow nine months and Lake Baikal six months. In Fig 1, the fall-out rates were corrected for the average latitudinal precipitation rate following the consideration that at a given latitude the ^{36}Cl fall-out is proportional to the precipitation rate.

The Risø sample is considered to be contaminated by a strong ^{36}Cl source in the laboratory. The fall-out rates show a strong latitudinal dependence with small rates of about 40 ^{36}Cl atoms/m^2 s at the pole regions, about thousand ^{36}Cl atoms/m^2 s at mid latitudes between 30 and 50° and about 400 ^{36}Cl atoms at the equator.

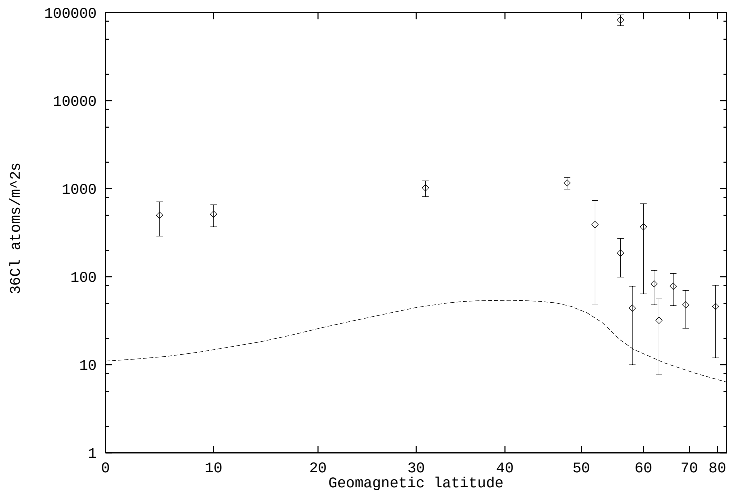

Fig. 1: Calculated ^{36}Cl fall-out with respect to the geomagnetic latitude

Predicted values of the average ^{36}Cl fall-out rate are in the range of 11 [1] and 17 (sun spot minimum) to 26 (maximum) ^{36}Cl atoms/m^2 s [2]. Fig. 1 also shows the prediction according to an average fall-out rate of 20 ^{36}Cl atoms/m^{2}s folded with the latitudinal dependence obtained from ^{90}Sr bomb fall-out data. Comparing measured and predicted values one sees that (1) the measured values are by a factor of about thirty larger than the predicted ones and (2) the latitudinal fall-out patterns are different. The reasons for the discrepancies are not clear. More samples shall be measured in order to avoid local effects. The latitude dependences could be different because ^{36}Cl as halogen element appears essentially as HCl where ^{90}Sr as earth alkaline element is attached to aerosols. ^{10}Be measurements of the same samples at the ETH Zürich will show whether this interpretation is correct.

For reliable calculations of the cosmogenic production of ^{36}Cl, it is necessary to know the relevant cross sections. For this reason, two irradiations of an Ar target have been performed with protons : one with 1 GeV protons at the SC at St. Petersburg, and the other with 28 MeV protons at the Munich accelerator laboratory. The results are

$$\sigma(^{40}\mathrm{Ar(p,2p3n)}^{36}\mathrm{Cl}) = 22 \pm 4\,\mathrm{mb\ at\ 1\ GeV}$$
$$\sigma(^{40}\mathrm{Ar(p,\alpha n)}^{36}\mathrm{Cl}) = 9 \pm 3\,\mathrm{mb\ at\ 28\ MeV}$$

Other measurements at energies between 50 and 100 MeV shall be performed at PSI Villigen (CH).

[1] D. Lal, B. Peters, Cosmic Ray produced Radioactivity on Earth, Handbuch der Physik **46/2** (1967) 551

[2] H. Oeschger, J. Houter, H. Loosli, M. Wahlen, 12th Nobel Symposium (1969) 471

2.4.2 Cosmogenic ^{26}Al in the lithosphere

G. Korschinek, G. Morteani [a], S. Neumaier, E. Nolte, E. Strack,
[a] Institute of Applied Mineralogy and Geochemistry, TUM, Garching

The knowledge of erosion rates is important for two reasons, among others : (1) in geochemical experiments as solar neutrino experiments , the contribution of background events is a function of depth and erosion rate and (2) the transformation of anhydrite into gypsum depends on the interplay of hydratization and uplift history and by these means on the erosion rate. The second point is very important for the gypsum industry.

Since the production rate of cosmogenic radioisotopes decreases with the depth, this relation can be used to determine erosion rates. In the first few meters of the earth crust, radioisotopes are mainly prfoduced by spallation and nuclear reactions of the nucleonic component of the cosmic radiation. Below this depth, muon induced reactions are dominant. In the case of ^{26}Al (5^+ $T_{1/2}$ = 716,000 y), these are the reactions $^{28,29,30}\mathrm{Si}(\mu^-,\nu_\mu xn)^{26}\mathrm{Al}(5^+)$, x = 2, 3 and 4. The dominant reaction is $^{28}\mathrm{Si}(\mu^-,\nu_\mu 2n)^{26}\mathrm{Al}(5^+)$. Since the production rate P(x) decreases almost exponentially with the depth x : $P(x) = P(x_o) \cdot^{-\frac{(x-x_o)}{\Lambda}}$ (Λ penetration depth), for erosion rates ε constant over the life time τ of the radioisotope this rate is calculated to be

$$\varepsilon = \frac{P(x_o)\cdot\Lambda}{N(x_o) - P_{bg}\cdot\tau} - \frac{\Lambda}{\tau}$$

x_o actual depth
P_{bg} background production rate.

Considered radioisotopes are ^{36}Cl in limestone $CaCO_3$ [1], ^{26}Al in quartz SiO_2 and ^{53}Mn in pyrite FeS_2. ^{36}Cl has an easy chemistry and is easily detectable but the contributions of $^{35}\mathrm{Cl}(n,\gamma)$ reactions depend on the elemental composition of the mineral and exchange of ^{36}Cl by meteoric ^{36}Cl has always to be considered. The physical and chemical preparation of the ^{26}Al samples is difficult. On the other hand, the use of ^{26}Al has three advantages:

(1) no exchange of ^{26}Al is expected, (2) there are no (n, γ) reactions contributing and (3) background production by e.g. U and Th is negligible. ^{53}Mn has similar advantages but is close to the detection limit.

Raw quartz samples from pre-drill cores of KTB from Weißenstadt and Egerer Waldhäusl were cut into small pieces of about 1 mm diameter and were analyzed by XRF and XRD. The small grains were selected and separated optically under the microscope, as well as magnetically and chemically. The obtained cleaned quartz samples were milled to a mesh size of 150 to 300 mesh, cleaned again chemically with ortho phosphoric acid and dissolved in HF : $SiO_2 + 4HF \rightarrow SiF_4 + 2H_2O$.

The fall-out of AlF_3 was converted chemically to $Al(NO_3)_3$ with HNO_3 and finally to Al_2O_3 by heating to 900 ° C. The Al_2O_3 samples were analyzed by ams. The results are shown in Fig. 1.

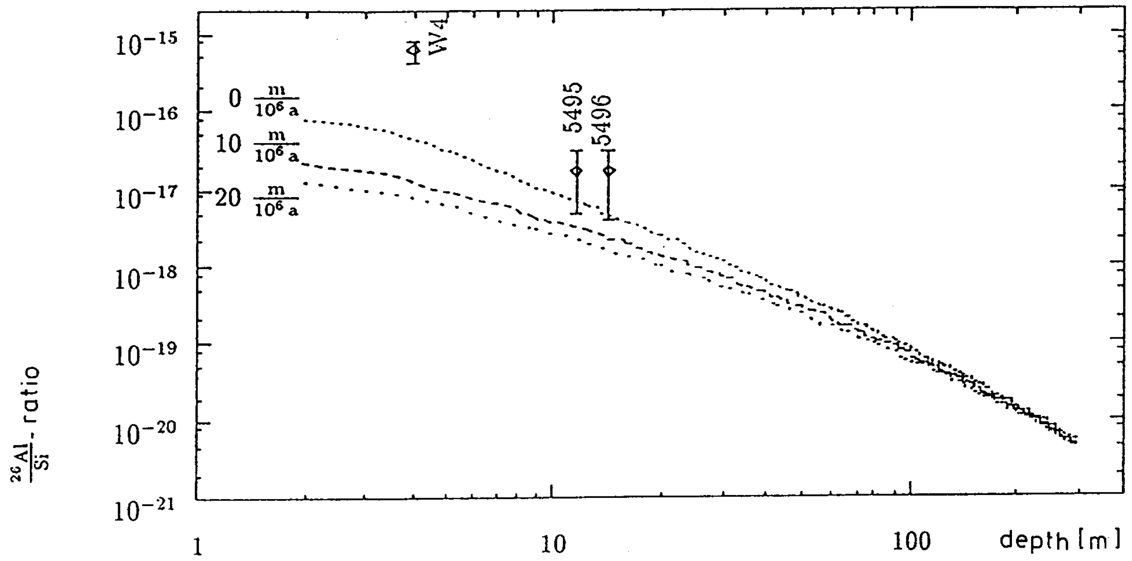

Fig. 1: Measured ratios of quartz samples from Weißenstadt and Egerer Waldhäusl (pre-core drills from KTB) and calculated ratios for the reaction $^{28}Si(\mu^-, \nu_\mu 2n)^{26}Al$ for different erosion rates. Reactions of the nucleonic component of the cosmic radiation were not taken into account. These are considered to contribute for the measured value to a depth of 4 m.

In order to be able to calculate the production rate of $^{26}Al(5^+)$ by the cosmic μ^- induced reaction $^{28}Si(\mu^-, \nu_\mu 2n)$, a quartz sample was irradiated with slow muons at PSI Villigen (CH). The production rate P of $^{26}Al(5^+)$ is given by

$$P = I_{\mu^-} \cdot f_C \cdot f_D \cdot f_I \cdot f_{2n} \cdot f_{(5^+)}$$

with

I_{μ^-}	flux of stopped negative muons
f_C	chemical compound factor (Si in SiO_2 : 0.30)
f_D	capture probability in the Si nucleus (0.651)
f_I	isotopic abundance (0.9223)
f_{2n}	probability for two neutron emission
$f_{(5^+)}$	probability for the population of the 5^+ ground state

The product $I_{\mu^-} \cdot f_C$ was obtained by measuring the muonic X radiation in silicon, $^{26}Al(5^+)$ was measured by ams in Munich. From this, the product $f_{2n} \cdot f(5^+)$ is deduced to be 0.026 ± 0.003. The relative strength of the 2n channel was calculated to be 0.184 [2]. This means that the 5^+ ground state is populated to only 14 %, 86 % go the isomeric 0^+ state. This fact is not so surprising, since in the muon capture reaction (μ^-, ν_μ), the emission of two neutrons and the γ deexcitation no large spins are transferred. With the help of this cross section, the production of ^{26}Al in the earth crust by muons can be calculated. The results for different erosion rates are also drawn in Fig. 1. The calculated values agree well with the measured ones for depth below 10 m. In the calculation, reactions of the nucleonic component ofthe cosmic radiation were not considered. These are considered to contribute for the measured $^{26}Al/Si$ value at 4 m.

[1] B. Dockhorn, S. Neumaier, F. J. Hartmann, C. Petit-Jean, H. Faestermann, G. Korschinek, H. Morinaga and E. Nolte, Z. Physik **A341** (1991) 117

[2] P. Singer, Lett.Nuov.Cim. **23** (1962) 669

2.4.3 ^{53}Mn and ^{59}Ni AMS measurements of meteorites

T. Faestermann, K. Knie, G. Korschinek, W. Müller, E. Nolte, W. Rühm, L. Zerle

During the period between the formation and their fall, meteorites are irradiated by interplanetary cosmic rays, which mainly consist of high-energetic protons. Induced by spallation reactions and by secondary produced neutrons, numerous isotopes are formed. Especially the long lived radio isotopes are important for the determination of exposure histories. For this reason we have measured the radionuklides ^{53}Mn ($T_{\frac{1}{2}} = 3.7 \cdot 10^6$ a) and ^{59}Ni ($T_{\frac{1}{2}} = 7.5 \cdot 10^4$ a) in the meteorites Jilin and Admire.

^{53}Mn measurements were performed by means off the two post accelerators (SchweIN) and a Bragg-chamber-detector [1]. The ^{59}Ni-concentration was determined in the gas-filled Q3D-spectrograph [2].

For the preparation of the AMS-targets, about 1–2 g of the meteorite was dissolved in HF under a pressure of 12 bar and a temperature of 185 °C for 10 h. As the concentration of Mn in Chondrites is only about 0.23% we have added 20 mg of carrier to handle the chemical separation. A small amount of the fluorides was taken off before, for neutron activation analysis of the Mn content. The obtained fluorides were separated by ion-exchange chromatography, which also performs the necessary suppression of the ^{59}Co for the Q3D-Measurement of ^{59}Ni. The Mn-fraction was prepared to MnO and the Ni-fraction to NiO which are appropriate targets for the high current ion source.

^{53}Mn is mainly produced by spallation on the target element Fe. Examples are the reactions ^{54}Fe(p,2 p)^{53}Mn, ^{54}Fe(n,p n)^{53}Mn, ^{56}Fe(p,2 p 2 n)^{53}Mn or ^{56}Fe(n,p 3 n)^{53}Mn. For this reason it is useful to give the concentrations in $\left[\frac{\mathrm{dpm}}{\mathrm{kg_{Fe}}}\right]$. According to the results of the AMS-Measurements and the neutron activation analysis we got the in table 1 shown specific concentrations:

Sample	$\frac{^{53}Mn}{^{55}Mn}$	specific concentration $\left[\frac{\mathrm{dpm}}{\mathrm{kg_{Fe}}}\right]$
Jilin S	$1.7 \pm 0.6 \cdot 10^{-10}$	86.2 ± 31
Jilin B	$4.8 \pm 2.0 \cdot 10^{-11}$	13.9 ± 5.8
Jilin VI	$2.9 \pm 1.8 \cdot 10^{-10}$	9.9 ± 6.1
Jilin V	$< 2.1 \cdot 10^{-10}$	< 7

Table 1: ^{53}Mn–Concentrations of the measured meteorites

As ^{53}Mn has a half life of more then 3 million years, the measured concentrations show the equilibrium distribution of an earlier status of the irradiation history. In that time the present surface was at different depths under the surface of the parent body, therefore the measured saturation activities differ by the factor 10.

^{59}Ni is a typical (n,γ)-product, from secondary neutrons induced by cosmic protons. The build up and the thermalisation of the neurons need a certain range, so the neutron flux and therefore the ^{59}Ni-production rate increase, until a certain size, with the depth under the preatmospheric surface and with the mass of the meteorite. For the meteorite Jilin we were able to confirm this by measuring two samples of different depths as indicated in table 2. The comparison of the specific concentrations for two different types of meteorites like Jilin (H Chondrite) and Admire (Pallasite) show the agreement of the saturation activities, which only depend of the neutron flux.

Sample	$\frac{^{59}Ni}{Ni}$	A$[\frac{dpm}{kg_{Ni}}]$
Jilin S	$2.4 \pm 1 \cdot 10^{-11}$	3398 ± 1000
Jilin B	$3.9 \pm 1 \cdot 10^{-11}$	5522 ± 1400
Admire	$3.7 \pm 1.1 \cdot 10^{-11}$	5239 ± 1550

Table 2: Activities of the measured meteorites

[1] J. Heinzl, G. Korschinek, H. Morinaga, E. Nolte, E. Preisenberger, U. Ratzinger, A. Urban, P. Dragovitsch, S.Vogt, Jahresbericht 1986, p. 69

[2] B. Bante, T. Faestermann, A. Gillitzer, S. Kastel, K. Knie, G. Korschinek, D. Müller, Jahresbericht 1991, p. 90

2.4.4 AMS measurement of a simulated lunar ^{59}Ni depth profile

T. Faestermann, S. Kastel, K. Knie, G. Korschinek, D. Müller, W. Spiegel [a]

[a] Institut für angewandte Mineralogie und Geochemie, TU München

^{59}Ni ($T_{\frac{1}{2}}$=95,000 a) in extraterrestrial matter can be produced by cosmic protons (^{60}Ni(p,pn)^{59}Ni, ^{59}Co(p,n)^{59}Ni), secondary cosmic neutrons (^{58}Ni(n,γ)^{59}Ni, ^{60}Ni(n,2n)^{59}Ni) and cosmic α–particles via ^{56}Fe(α,n)^{59}Ni. By a very low Ni– and Co–content ^{59}Ni is exclusively produced by α–particles. Because of decreasing cosmic ray flux with increasing energy most ^{59}Ni is produced near the surface by low energetic solar α–particles ($\approx$50% in the top 0.2 mm). Therefore the measurement of a ^{59}Ni–depth–profile allows a determination of the mean solar α–flux over the last few 100,000 a [1]. As the surfaces of meteorites are ablated during entering the earth's atmosphere, only samples of the moon are suitable.

In order to get a realistic experimental normalization a depth profile was simulated. Appropriate sets of three approximately 0.2 mm (65 mg/cm^2) thin stone slices were irradiated with α–particles of 15, 20, 26, 33 and 41 MeV respectively. To obtain information about eventual inhomogeneities in the samples or an inconstancy of the irradiation current, ^{57}Ni ($T_{\frac{1}{2}}$=36 h) was determined too. It is produced by the reaction ^{54}Fe(α,n)^{57}Ni with a similar energy dependence of its cross section and can be measured easily with a GeLi–detector.

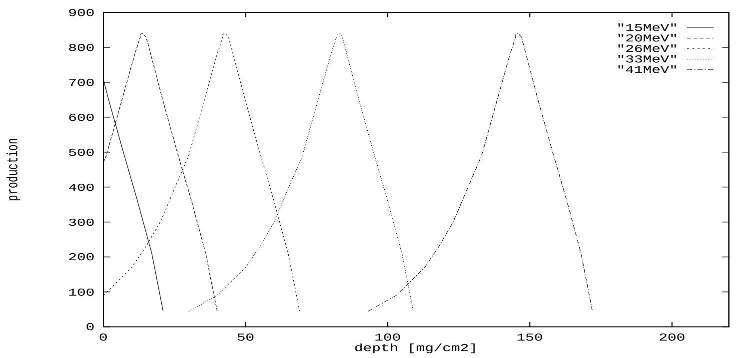

Fig. 1: Calculated production rates of several energies (arbitrary units) versus the depth (mg/cm^2)

To get samples for an AMS–measurement, the slices and each 20 mg Ni carrier were disolved in hydro fluoric acid at 100 bar and 200 °C. Then cobalt, the disturbing stable isobar, was suppressed to approximately 100 ppb by ionexchangechromatography. The ^{59}Ni/Ni ratios in the precipitated NiO, measured with the gasfilled Q3D–spectrograph as described in [2], were between 1×10^{-12} and 5×10^{-11}. From these concentration we can estimate an expected ^{59}Ni/Ni ratio of 1.1×10^{-12} in the top sample of lunar rock 74275 (0-0.5 mm). The value of the next layer (1-1.5 mm) can be calculated to 4×10^{-14}. The expected ^{59}Ni–concentration of the top layer is one order of magnitude above our present detection limit of 1×10^{-13} [2].

[1] L.J. Lanzerotti, R.C. Reedy, J.R. Arnold, Science **179** (1973) 1232

[2] B. Bante, T. Faestermann, A. Gillitzer, S. Kastel, K. Knie, G. Korschinek, D. Müller, Jahresbericht 1991, p. 90

2.4.5 A new half-life determination of ^{59}Ni

K. Knie, G. Korschinek, E. Nolte, W. Rühm, H. Vonach [a], D. Weselka [b], L. Zerle

[a] Institute of Radium Research, University of Vienna, Vienna, Austria

[b] Institute of High Energy Physics, Austrian Academy of Sciences, Vienna, Austria

The half-life of ^{59}Ni was determined by two ways : (1) by a relative measurement of the radioactivities ^{59}Ni and ^{55}Fe produced by (n_{th}, γ) reactions and (2) by comparing activity and ams measurements of samples from the meteorite Admire.

(1) Enriched ^{58}Ni metal powder (99.89 %) and an enriched ^{54}Fe metal foil (99.8 % , 0.5 mg/cm^2 thick) were irradiated by thermal neutrons at the Munich research reactor. ^{59}Ni and ^{55}Fe where produced via thermal neutron capture reactions (n_{th}, γ) with cross sections taken to be 4.6 b and 2.25 b, respectively. ^{55}Fe served for the normalization of the neutron dose and as efficiency calibration standard for the detector. The Ni sample was cleaned chemically, reduced to metal, melted and rolled to a foil of 1.18 mg/cm^2 thickness. The radioactivities ^{59}Ni and ^{55}Fe were measured with a silicon detector. The spectra are shown in Fig. 1. Both radioactivities decay by electron capture emitting K_α and K_β X-radiation of 6.93 and 7.65 keV (^{59}Ni) and of 5.89 and 6.49 keV (^{55}Fe), respectively. The final result is $T_{1/2}(^{59}\mathrm{Ni})$ = 96,000 ± 12,000 y. This values is somewhat larger than the value of 76,000 ± 5,000 y of Nishizumi [1] where activity and number of nuclei of ^{59}Ni were measured. It should be pointed out that our experiment is a relative measurement where the errors in neutron dose and efficiency calibration do not contribute.

(2) The life time of a radioisotope is given by the ratio of the number N of nuclei and the activity A : τ = N/A. From a sample of the metal phase of the meteorite Admire that, in this phase, has a nickel content of 10.7 % [2], measurements of A and N were performed. The activity measurement yielded 5.0 ± 0.5 bq/kg [3] and the ams measurements performed at Argonne National Laboratory and at the Munich accelerator laboratory gave $[^{59}\mathrm{Ni}]/[\mathrm{Ni}] = (2.3 \pm 0.4) \cdot 10^{-11}$ [4] and $(3.7 \pm 1.1) \cdot 10^{-11}$ [5], respectively. Taking the ratio of activity and average of the ams measurements, a half-life of 118,000±22,000 y is obtained. This value compares well with our half-life result, but is only within two standard deviations consistent with the result of [1].

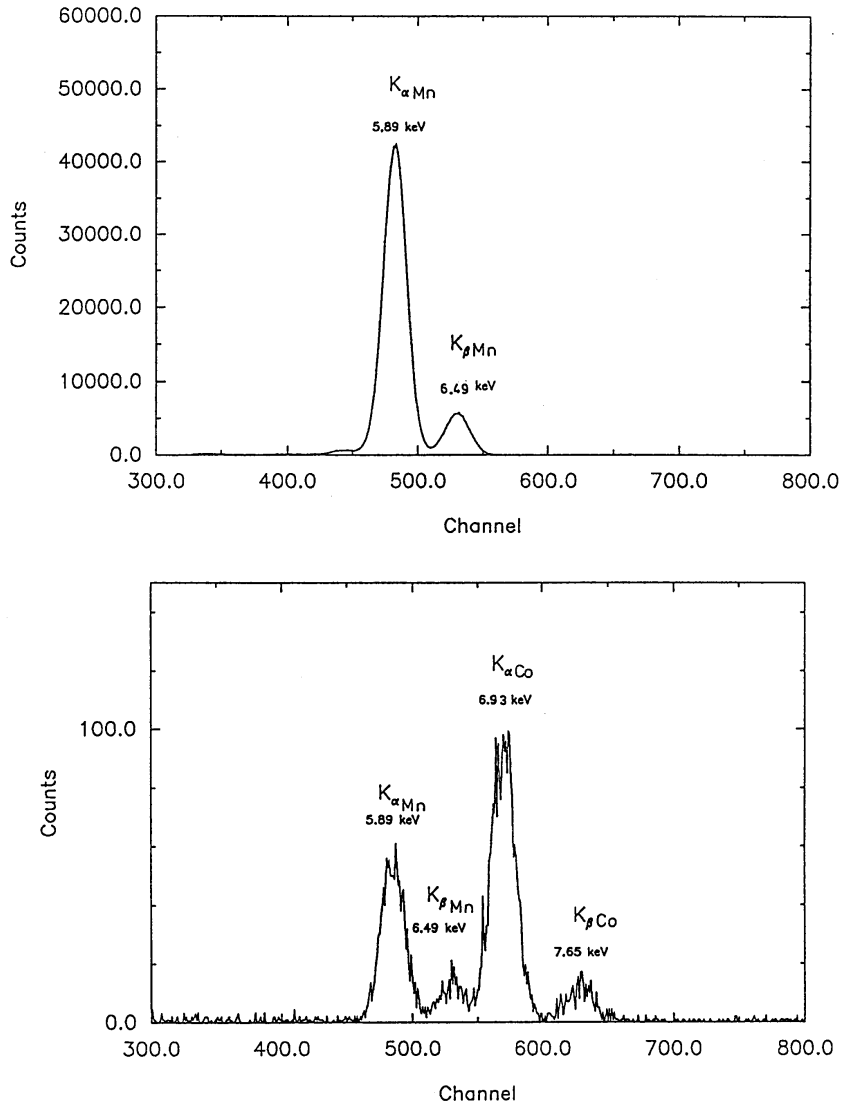

Fig. 1: X-ray spectra taken with a silicon detector from the ^{59}Ni and ^{55}Fe radioactivities

[1] K. Nishiizumi, R. Gensho and M. Honda: Radiochim. Acta 29(1981)113
[2] P.R. Buseck and J.I. Goldstein, Geological Society of America Bulletin 80 (1969)2141
[3] M. Honda and J.R. Arnold : Science 143 (1964) 203
[4] W. Kutschera, L. Ahmad, B. G. Glagola, R.C. Pardo, K.E. Rehm, D. Barkovits, M. Paul, J.R. Arnold and K. Nishiizumi : to be published in Nucl. Instr. and Meth. A
[5] K. Knie : Diploma thesis 1992, Technical University of Munich

2.4.6 Medical applications of Accelerator Mass Spectroscopy with ^{26}Al

P.Gerisch, G.Korschinek, E.Nolte, W.Rühm, and T.H.Ittel [a]
[a] Med. Fakultät RWTH Aachen

In spite of its abundant occurrence in the earth crust (8% of weight) very little is known about aluminum-toxicity. Aluminum containing medicaments have a wide application in medicine. Especially in Nephrology, aluminium containing medicaments are used. The kidneys control calcium and phosphate metabolism, and eliminate aluminum too. Renal patients are not able to eliminate aluminium and in addition they receive large quantities of aluminum containing drugs for phosphate-binding. Therefore, they have increased aluminum concentration in serum. Aluminum related disorders are renal osteodystrophy [1], dialysis encephalopathie [2] and microcytic anaemia [3].

Conventionally tracer methods can't be used for examination of aluminum metabolism because of the unsuitable half-lives of aluminum isotopes (^{23}Al $T_{1/2}$=470ms, ^{24}Al $T_{1/2}$=2.07s, ^{25}Al $T_{1/2}$=7.18s, ^{26}Al $T_{1/2}$=716000a, ^{28}Al $T_{1/2}$=2.246min, ^{29}Al $T_{1/2}$=6.6min).
For medical application the only possible isotope is ^{26}Al ($T_{1/2}$=716000a). It decays by 82% β^+ emission and to 15% by electron capture to ^{26}Mg. The long half-live of 716000 years means that radioactivity for once incorporated ^{26}Al decreases only with the biological half-live of aluminum. AMS is a versatile tool for detection of smallest amounts of ^{26}Al, so that the obtained radiation doses are neglegible.

For testing chemical and physical processing and detection of ^{26}Al, blood and urin samples of 5 Sprague-Dawley rats had been measured. Two nephrectomised rats (5/6 of the kidneys had been removed) and three normal rats received an oral dose of 20 ng ^{26}Al and 0.2mg and 10mg, respectivly, of ^{27}Al as aluminumchloride solution. Blood samples were taken after 0, 2, 5, 24 hours. Urin was collected over 24 hours. 10 mg of aluminum was added as carrier to the blood samples, 100mg to the urin samles.

^{26}Al - detection

For detection of ^{26}Al a ΔE-E detector consisting of a ionisation chamber and a silicium surface barrier detector was used. The detection limit for ^{26}Al/^{27}Al-ratios is $3 * 10^{-15}$ [5].

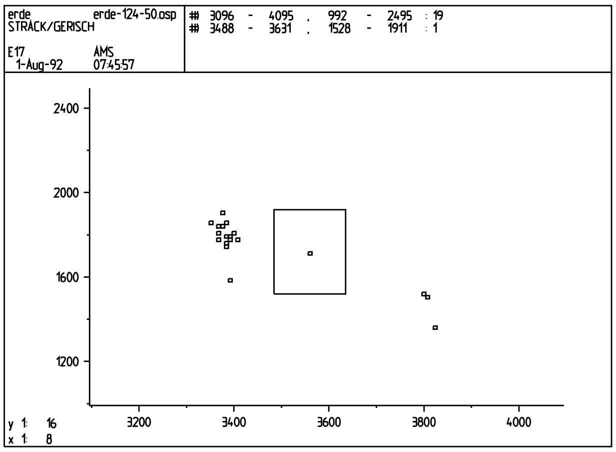

Fig. 1: Two-dim. spectrum of a magnesium-containing sample measured with ΔE-E detector with Wien-filter, horizontal ER, vertical dE, arbitrary units; left ^{27}Al, middle ^{26}Al, right ^{26}Mg

Pharmacokinetics

Changes of Al concentrations are treated as reactions of first order. The concentration of ^{26}Al in blood is described by two models.

(1) One-compartment model:

The body consists of one compartment (Fig. 2). Aluminum is absorbed with the absorption constant k_a and eliminated with the elimination constant k_{el}, from one compartment. The solution of the one-compartment model is the Bateman function (??). For a given k_a Al concentrations in blood vary with k_{el}, smaller values of k_{el} cause higher Al concentration c(t) in blood.

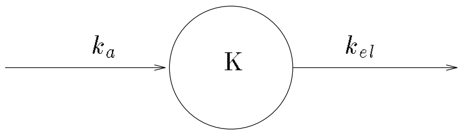

Fig. 2: Open One-compartment model

$$C(t) = \frac{D}{V} \cdot \frac{k_a}{k_a - k_{el}} \cdot (e^{-k_{el} \cdot t} - e^{-k_a \cdot t}) \tag{24}$$

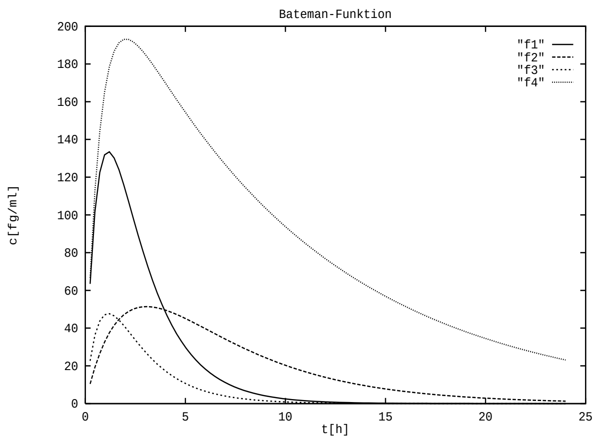

Fig. 3: Bateman-function with different k_a, k_{el}
f1: $k_a = 1.4\,h^{-1}$ $k_{el} = 0.5\,h^{-1}$
f2: $k_a = 0.2\,h^{-1}$ $k_{el} = 0.5\,h^{-1}$
f3: $k_a = 0.5\,h^{-1}$ $k_{el} = 1.4\,h^{-1}$
f4: $k_a = 1.4\,h^{-1}$ $k_{el} = 0.05\,h^{-1}$

(2) Two-compartment model:

Absorption and elimination of the aluminum between stomach, blood, organs and urin are described by the constantsλ_a, a1, a2 a3 and a4 respectively (Fig. 4 and 5). a4 is the elimination constant describing the renal-function. The rate constants a_i can be described by half-lives T_i=ln(2)/a_i. λ_a is the ratio of the Al absorbed by the blood to Al in the stomach. From measured urin and blood samples λ_a is estimated to be about 10^{-4}, in agreement with Barker and Day [4]. T_1 describes absorption from stomach to blood, T_2 from blood to organs, T_3 from organs to blood, T_4 from blood via kidneys to urin. The solution of the two-compartment model is equation (25), with c_i=$c_i(\lambda_a, a_i)$, $\vec{u_i} = \vec{u_i}(a_i)$.

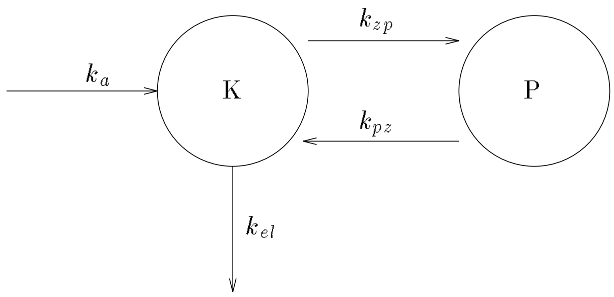

Fig. 4: Open two-compartment-model

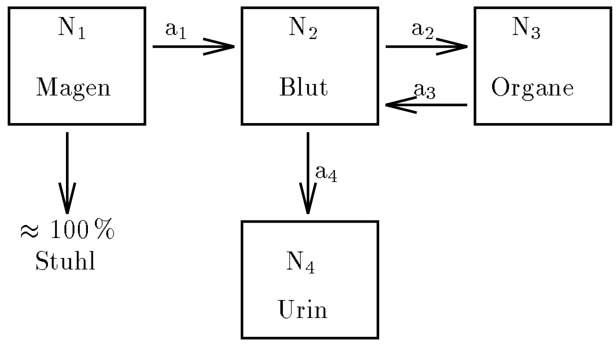

Fig. 5: The Two-compartment model for aluminum

$$\vec{N}(t) = c_1 \cdot \vec{u_1} \cdot e^{\lambda_1 \cdot t} + c_2 \cdot \vec{u}_2 \cdot e^{\lambda_2 \cdot t} + c_3 \cdot \vec{u}_3 \cdot e^{\lambda_3 \cdot t} \tag{25}$$

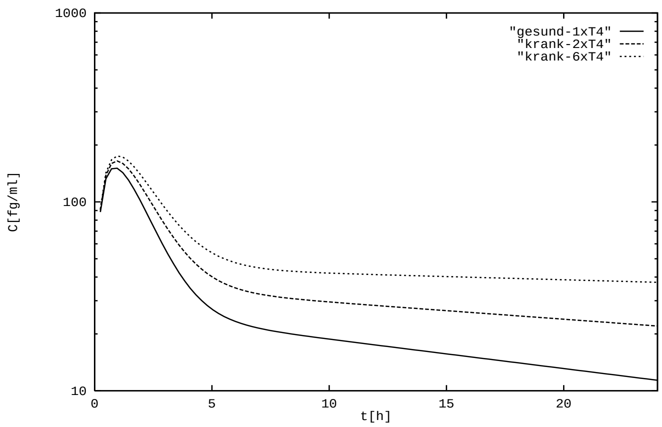

Fig. 6: Solution of the two-compartment model for Al concentration in blood with different a4 to simulate normal and insufficient renal-function

The two-compartment model shows, that insufficient renal function causes higher ^{26}Al concentration in blood, especially after 24 hours. For large values of T_3 the two-compartment model reduces to be the Bateman-function of the one-compartment model.

Results

The blood samples were measured to have $^{26}Al/^{27}Al$-ratios between $1.1 * 10^{-12}$ and $5.6 * 10^{-14}$ and urin samples between $3.8 * 10^{-13}$ and $7.5 * 10^{-14}$. Figures (7) and (8) show that nephrectomised rats have higher ^{26}Al-concentration in blood than normal rats. The two-compartment model gives essential results, but it does not explain the measurements quantitatively. The experiment should be repeated with more blood samples taken and more rats.

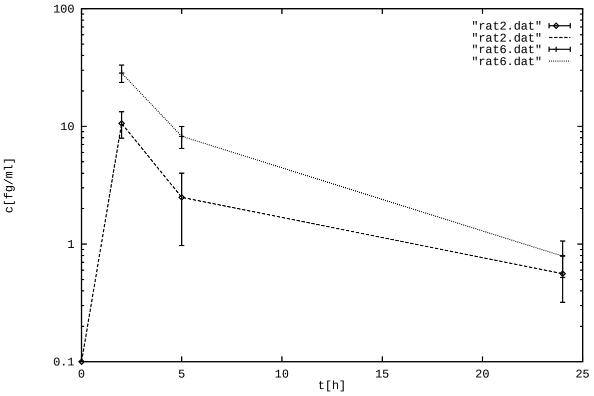

Fig. 7: Rat 2a (normal) and rat 6a (nephrektomized), both 0.2 mg Al

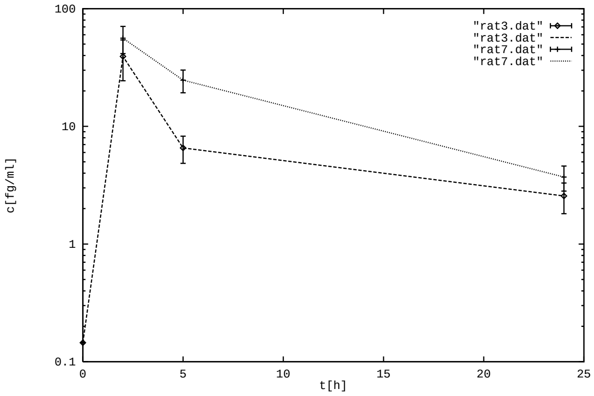

Fig. 8: Rat 3a (normal) and rat 7a (nephrektomized), both 10 mg Al

This work has been funded by BMFT.

[1] S. M. Ott, N.A. Maloney, J.W. Coburn, A.C. Alefrey, N. Eng. J. Med. **307** (1982) 709

[2] A. C. Alfrey, G. R. LeGendre, W. D. Kaehny, N. Eng. J. Med. **294** (1976) 184

[3] R.J.S. McGonigle, V. Parson, Nephron **39** (1985) 1

[4] J.P. Day, J. Barker, L.J.A. Evans, J. Perks, P.J. Seabright, P. Ackrill, J.S. Lilley, P.V. Drumm, G.W.A. Newton, The Lancet **337** (1991)

[5] P. Gerisch, Diplomarbeit TUM

2.4.7 Neutron transport calculations and the dosimetry system DS86

W. Rühm, G. Korschinek, H. Morinaga, E. Nolte, K. Kato [a]
[a] Suzugamine Womens' Junior College, Inokuti, Nishiku, Hiroshima, Japan

The neutron spectrum of the Hiroshima A-bomb is basis of the Dosimetry System 1986 (DS86). To reconstruct this spectrum we are investigating a gravestone made of granite located 107 m from the hypocenter of the explosion.

Five radioisotopes produced via (n,γ) - reactions by neutrons from the atomic explosion were identified up to now: ^{36}Cl and ^{41}Ca by accelerator mass spectrometry at our Tandem laboratory ([1], [2]), ^{60}Co ([3]), ^{152}Eu ([4]) and ^{154}Eu ([3]) by gamma spectroscopy. It turns out that the measured activities of these isotopes cannot be explained by the DS86 - neutron spectrum but by a much harder neutron spectrum ([5]).

To interpret the measurements mentioned above neutron transport calculations were performed with the Monte Carlo programm MORSE (**M**ultigroup **O**ak **R**idge **S**tochastic **E**xperiment) on a Cray Y-MP. As first step the chemical composition of the gravestone and the cross sections used for the calculations were tested. For this the irradiation of a similar granite with thermal neutrons at the Research Reactor Garching ([6]) was simulated with MORSE. The measured activations of gold foils as function of depth in the granite could be reproduced by the calculation within the errorbars as can be seen from figure 1.

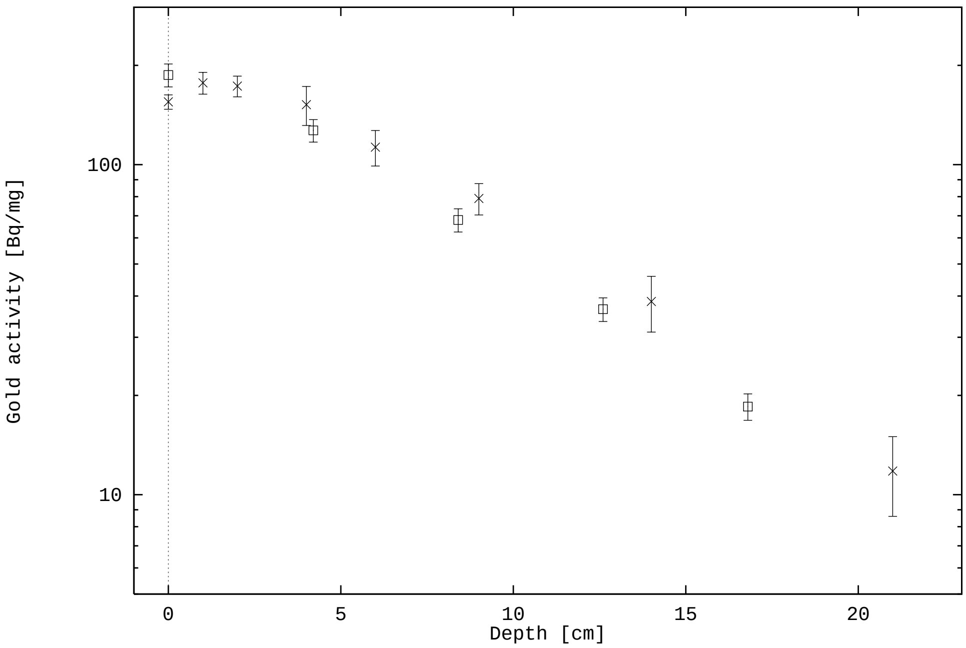

Fig. 1: Measured (□) and simulated (×) gold depth profile.

The same situation takes place when an irradiation with a hardened fission spectrum is simulated. The measured ^{58}Co - activities of Ni - probes as function of depth in the granite agree within the errorbars with a MORSE simulation.

As next step, the DS86 neutron spectrum was checked by a MORSE simulation. In DS86, the transport program DOT-IV was used for the calculation using an energy binning of 44 groups up to an energy of 19.6 MeV. The first group ranges from 10^{-5} eV to 0.414 eV ([7]). As for the MORSE calculation, 19 energy groups up to an energy of 0.414 eV were used due to the importance of this energy range for neutron activation. A simple air over ground geometry was used and importance sampling and a pointdetector positioned 107 m from the hypocenter at the gravestone site as flux estimator were applied. Soil and air composition, burst height of 580 m and bomb strength of 15 kt were taken from DS86 served as input parameters. As reported in the last annual report, the MORSE simulation and the DS86 calculation are in agreement within the statistical uncertainties for energies above 0.414 eV. For energies below 0.414 eV, MORSE resolves a Maxwell Boltzmann part due to the 19 energy groups used ([8]).

In the next calculation, granite was used as soil since the granitic gravestones are close to each other in this Japanese grave yard. Figure 2 shows the result compared to the neutron spectrum from the calculation using DS86 soil: the spectrum becomes harder, there are less thermal but more epithermal neutrons. This is due to the low water content of granite which is about 30 times lower compared to the soil composition used for the DS86 calculations.

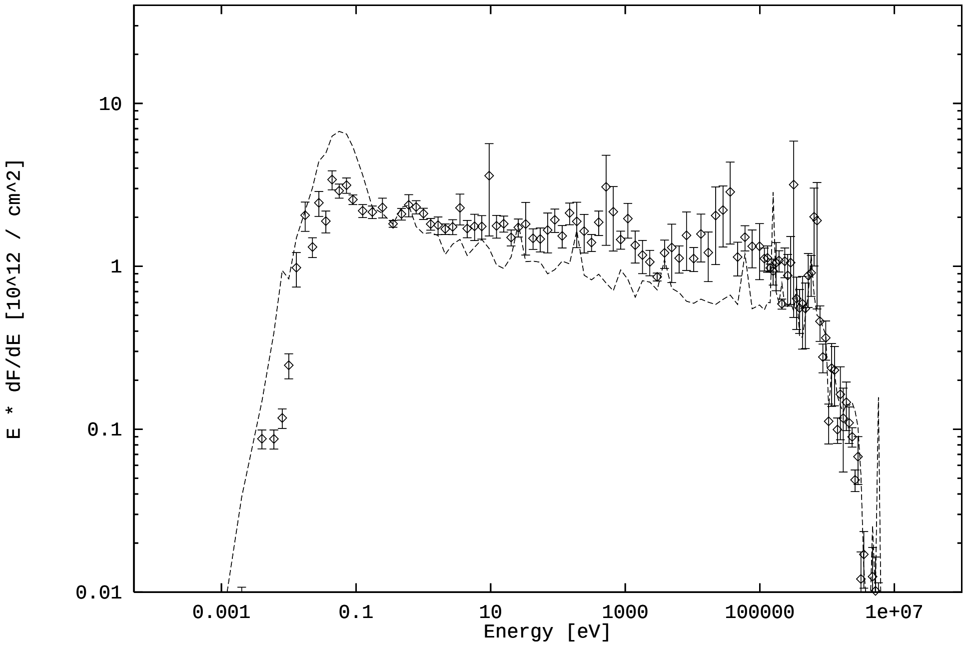

Fig. 2: Neutron fluences calculated with MORSE: DS86 input (lines) and granitic soil (errorbars).

By folding this neutron spectrum with the corresponding (n,γ) cross sections, the effective thermal neutron fluences, defined as

$$F_{th,eff} \equiv \frac{^{(i+1)}N}{^{i}N} \cdot \frac{1}{\sigma_{i,th}}, \quad i = 35, 40, 59, 151, 153 \tag{26}$$

can be obtained for all radio isotopes mentioned above (see for example [2]). In figure 3 the effective thermal neutron fluences obtained from the calculation with granitic soil are compared to the experimental data. As seen from this figure the ^{36}Cl measurement cannot be explained by the simulation.

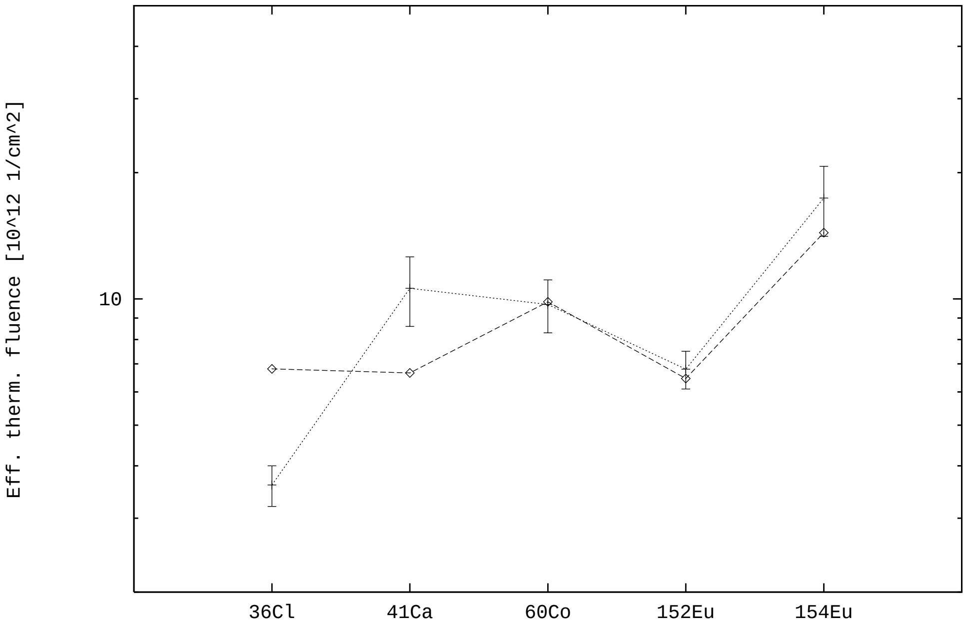

Fig. 3: Effective thermal fluences: comparison of measurement (errorbars) and MORSE - calculation (◇) with granitic soil.

Parameters which provide an additional hardening of the neutron spectrum (which is required to explain the measured effective thermal fluences) are harder source terms and less air humidity. For this reason a MORSE run with dry air (which was assumed in the Dosimetry System before DS86, T65D) and a fission source 580 m above ground was perfomed. The result is a neutron spectrum 1 m above ground (normalized to 15 kt and a neutron leakage of 0.177 mol/kt from DS86) which is much harder than the previous spectrum (see figure 4). However even this hardening is not enough to explain the discrepancy in the effective thermal neutron fluences between ^{36}Cl on one hand and ^{41}Ca and ^{152}Eu on the other.

Using the spectrum from figure 2 and a build up factor of 16 percent for thermal neutrons 1 cm inside the stone ([3]), the bomb strength can be used as fit parameter. A least square fit yields 9.6 kt for all isotopes and 14.7 kt for all isotopes without ^{36}Cl compared to (15 ± 3) kt which is assumed in DS86.

/noindent This work has been funded by BMFT and DFG.

[1] K. Kato, M. Habara, T. Aoyama, Y. Yoshizawa, U.Biebel, G. Haberstock, J. Heinzl, G. Korschinek, H. Morinaga, E. Nolte, Journal of Radiation Research **29** (1988) 261

[2] W. Rühm, K. Kato, G. Korschinek, H. Morinaga, E. Nolte, Z. Phys. **A341** (1992) 235

[3] K. Kato, private communication

[4] K. Kato, M. Habara, T. Aoyama, H. Sakata, Y. Yoshizawa, Japanese Journal of Applied Physics **29** (1990) 1546

[5] W. Rühm, K. Kato, G. Korschinek, H. Morinaga, A. Urban, L. Zerle, E. Nolte, Nucl. Instr. and Meth. **B52** (1990) 557

[6] U. Biebel, Diplomarbeit 1987

[7] W. C. Roesch, Editor, US - Japan Joint Reassessment of Atomic Bomb Radiation Dosimetry in Hiroshima and Nagasaki: final report, Radiation Effects Research Foundation (1987)

[8] W. Rühm, G. Korschinek, H. Morinaga, E. Nolte, K. Kato, Jahresbericht 1991, p. 86

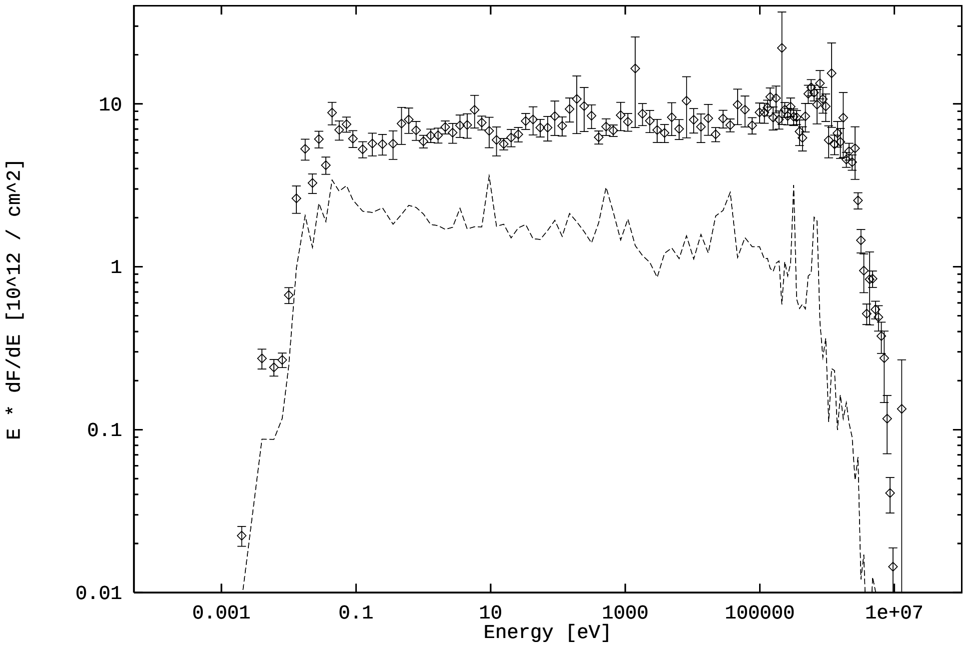

Fig. 4: Neutron fluences, calculated with MORSE: Granitic soil (lines) compared to granitic soil plus fission source plus dry air (errorbars).

2.4.8 Detection of ^{90}Sr by AMS

T. Faestermann, A. Gillitzer, S. Kastel, K. Knie, G. Korschinek, D. Müller and M. A. Kim [a]
[a] Institut für Radiochemie der Technischen Universität München

The long living nuclear fission product ^{90}Sr ($T_{1/2}$= 28.5 a) can get into the environment by nuclear weapon tests and accidents in nuclear power plants. Incorporated in the human body it replaces calcium in the bones and so has an effective halflife of about ten years in the body. Since it is a pure β emitter, the detection of ^{90}Sr is difficult and time-consuming. We studied the detection of ^{90}Sr with AMS as a fast alternative to the usual methods.

^{90}SrF$^-$ molecular ions are extracted from the high current sputter source and accelerated with a terminal voltage of 14 MV. For the separation of isobars we use the gasfilled Q3D magnetic spectrograph, while the background from stable isotopes is effectively suppressed by a time of flight setup [1].

For isobaric separation a high energy in the Q3D is desirable. Up to now 200 MeV ^{90}Sr ions lost 40 MeV in the Ni–foil, which separates the gasfilled volume from the vacuum, and in the foils of the stop detector of the time of flight path. This energy loss could be reduced to 10 MeV by a newly constructed parallel plate avalanche counter with 30 $\frac{\mu g}{cm^2}$ polyimide foils [2]. In addition a foil changing mechanism has been built, which allows to mount or remove quickly the foil separating the Q3D volume from the vacuum in the beam transport system. Therefore thin organic foils can be used, since they do not have to stand the macroscopic beam during the tuning.

For the measurements shown in the figures we used ^{90}Sr ions in the 12$^+$ charge state with an energy of 176 MeV because of the higher stripping yield. The figures show two dimensional spectra as

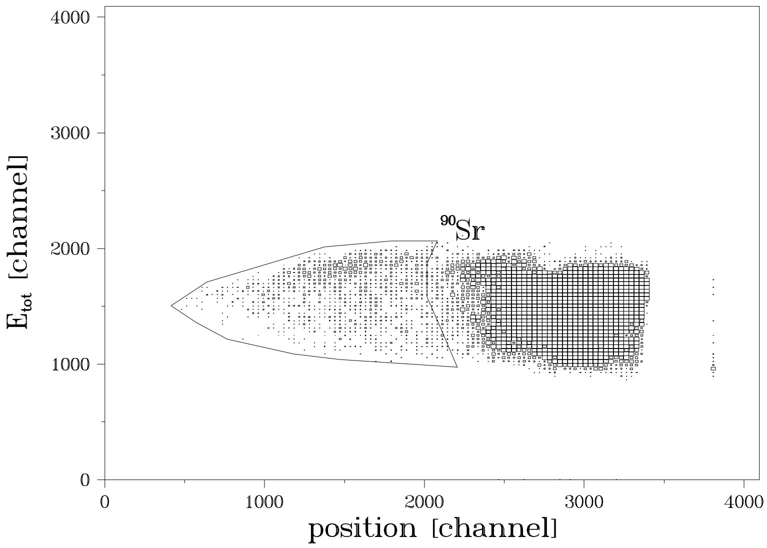

Fig. 1: Energy vs. position spectrum for 176 MeV ^{90}Sr ions from a calibration sample with a concentration of ^{90}Sr/Sr $= 10^{-8}$ after traversing the Q3D magnetic spectrograph filled with 1.6 mbar N_2. The measuring time was 330 s. The ^{90}Sr activity of this sample amounts to about 600 Bq.

a function of the energy and the position of the ^{90}Sr ions in the focal plane detector. The position is correlated to the magnetic rigidity, high channel numbers correspond to low magnetic rigidity.

The spectrum of a calibration sample with a concentration of ^{90}Sr/Sr $= 10^{-8}$ is shown in figure 1, in figure 2 the spectrum for a blank Sr sample. The dominant events are due to the stable isobar ^{90}Zr. The polygon indicates the area with the best signal to noise ratio for ^{90}Sr. The total transmission for ^{90}Sr ions from the Faraday cup in front of the accelerator up to the detection within this polygon amounts to 1.1 %.

With the small Zr content of the pure chemicals used as blank samples we can detect concentrations down to $3 \cdot 10^{-12}$ ^{90}Sr/Sr. For a typical sample quantity of 15 mg, which yields current for more than 20 h, this concentration corresponds to an activity of 0.2 Bq.

As environmental samples we measured Brazil nuts and two soil samples from the Ukraine. The very high Zr content in these samples limited our senitivity considerably, which was however high enough to detect ^{90}Sr contaminations below the EC guideline for food contamination (125 $\frac{Bq}{l}$).

The main emphasis in our work lies in a rapid detection scheme. Therefore we worked also on an optimization of the chemical procedures. The time needed to extract Sr from liquid environmental samples could be reduced from about 5 days to 8 hours by using a very fast method with ion exchanging resins and crown-ether-18-6 [3, 4].

A time consuming procedure is still the precipitation of SrF_2 as the last step. It also need a large amount of Sr carrier. Since we measure isotope concentrations, this limits our sensitivity for the measurement of the ^{90}Sr activity. The problem can be avoided by using $SrCO_3$ samples and extracting SrO^- ions. This should deliver an intensity similar to the extraction of SrF^- ions.

With this method about 8 h after taking liquid environmental samples the ^{90}Sr can be extracted as $SrCO_3$. In case of emergency the accelerator and the experimental setup could be prepared during this time and within about 24 h after an accident the ^{90}Sr activity could be determined with a sensitivity of a few $\frac{Bq}{l}$.

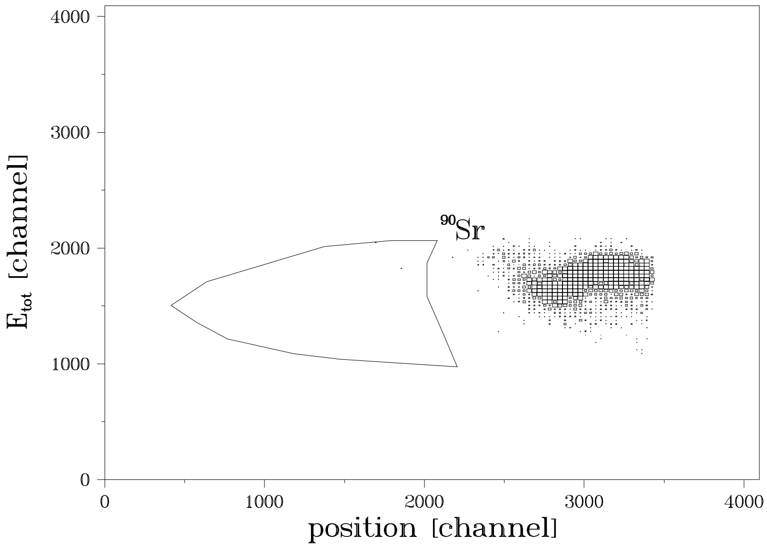

Fig. 2: Spectrum for ^{90}Sr ions from a blank Sr sample under the same conditions as in figure 1 and a measuring time of 3423 s

[1] B. Bante, T. Faestermann, A. Gillitzer, G. Korschinek, D. Müller, and U. Bittner, Jahresbericht 1990, p. 103

[2] G. Dollinger, W. Heimkes, P. Mayer-Komor, M. K. Nacke, Jahresbericht 1988, p. 170.

[3] D. Tait, A. Wiechen, W. Behrens, Die Milchwissenschaft 44 (10), p. 630, 1989

[4] S. Kastel, Diploma Thesis TUM, 1993

2.4.9 Large, small and artificial violations of the Pauli exclusion principle and the size of the electron

E. Nolte, M. Thoma [a]

[a] now at Institute for Theoretical Physics, Justus-Liebig University, Gießen

Considering eventual violations of the Pauli exclusion principle (PEP), one has to distinguish between (a) large violations of PEP, (b) small violations of PEP, and (c) superficial violations of PEP.

a) Large violations of PEP

In nature, two types of statistics are observed : Fermi-Dirac statistics (FD) and Bose-Einstein (BE) statistics. Particles with half-integer spin obey FD statistics and are called fermions, particles with integer spin obey BE statistics and are called bosons. Ensembles of two or more identical fermions are described by a wave function which is completely antisymmetric with respect to exchange. The wave function of an ensemble of two or more bosons is completely symmetric with respect to exchange. It follows that one state cannot be occupied by two ore more identical fermions whereas an infinite number of bosons can occupy one state.

In quantum theory, intermediate types of statistics are allowed. This subject is the matter of parastatistics (see e.g.[1]). One distinguishes para-Fermi and para-Bose statistics. In para-Fermi statistics of order 2 e.g., up to two identical particles can occupy one state and up to three identical particles can occupy one state in para-Fermi statistics of order three. Quarks can be considered to be fermions by introducing three colors or without introduction of colors they can be seen equivalently as para-fermions of order three. The question is whether it is always possible to remove para-statistics to FD or BE statistics by introducing an appropriate number of degrees of freedom.

b) Small violations of PEP

So far, there is no experimental or theoretical evidence for a violation of PEP. A limitation of PEP in this sense would be a small violation of PEP. Experimentally, we have looked with ams for small violations of PEP in atoms and nuclei by searching for atoms with three electrons in the K shell or for nuclei with three protons or three neutrons in the nuclear $1s_{1/2}$ shell. These non-Paulian atoms and nuclei are described with $\tilde{}$.

The results published in [2] were:

$$\frac{N(^{20}\widetilde{Ne})}{N(^{20}Ne)} < 2 \cdot 10^{-21}, \frac{N(^{36}\widetilde{Ar})}{N^{36}Ar)} < 4 \cdot 10^{-17}$$

for atoms and

$$\frac{N(\widetilde{^{5}Li})}{N^{6}Li)} < 8 \cdot 10^{-18}, \frac{N(\widetilde{^{5}He})}{N^{4}He)} < 2 \cdot 10^{-15}$$

for nuclei. The results for the non-Paulian nuclei $\widetilde{^{5}Li}$ and $\widetilde{^{5}He}$ can be discussed in the framework of the early nucleosynthesis in order to obtain a limit $\beta^2/2$ of having two protons or two neutrons in the symmetric state. The results are [3]

$$\frac{\beta^2}{2} < 2 \cdot 10^{-28} \text{ for protons and}$$

$$\frac{\beta^2}{2} < 2 \cdot 10^{-15} \text{ for neutrons.}$$

c) Superficial violations of PEP

In a recent paper [4] it is pointed out that in case the electron is a composite particle made out of a fermion w and a boson C electronic transitions from the 2 P to the 1 S state in atoms with small transition rates could occur violating PEP superficially for electrons though PEP is still valid for the constituent w. Such transitions could be described with a decay constant $\tilde{\lambda}$ which is connected with the electromagnetic decay constant λ_{em} by $\tilde{\lambda} = \frac{\beta^2}{2}\lambda_{em}$. The non-Paulian atoms would be produced according $N(\tilde{Z}) = N(Z) \cdot \tilde{\lambda}t$, where t is the average time from the nucleosynthesis to the time of formation of our galaxy, $t \approx 4.5 \cdot 10^9$y. With the measured numbers and with the life times λ_{em}^{-1} of 2.6 fs and 1.0 fs for the lifetime of a K hole in Ne and in Ar, respectively, we obtain [5]

$$\tilde{\lambda}^{-1} > 2 \cdot 10^{30} \text{ y (Ne) and } \tilde{\lambda}^{-1} > 4 \cdot 10^{27} \text{ y (Ar)}$$

as well as

$$\frac{\beta^2}{2} < 4 \cdot 10^{-53} \text{ (Ne) and } \frac{\beta^2}{2} < 8 \cdot 10^{-51} \text{ (Ar)}$$

for the probability of having two electrons in the symmetric state.

In [4], the transition rates $\tilde{\lambda}$ and λ_{em} are connected to the size of the electron:

$$\frac{\tilde{\lambda}}{\lambda_{em}} \approx 1.7 \cdot 10^{-50} (Z\, r_{e^-} [10^{-18}\ m])^6,$$

where Z is the atomic number and r_{e^-} is the radius of the electron.

From this relation we deduce the following limits for the radius of the electron:

$$r_{e^-} < 4 \cdot 10^{-20}\ m\ (Ne) \text{ and } r_{e^-} < 5 \cdot 10^{-20}\ m\ (Ar)\ .$$

[1] H.S. Green, Phys. Rev. **90** (1953) 270
[2] E. Nolte et al., Z. Physik **A340** (1991) 411
[3] M. Thoma and E. Nolte, Phys. Lett. **B291** (1992) 484
[4] K. Akama, H. Terazawa and M. Yasue, Phys. Rev. Lett. **68** (1992) 1826
[5] V.M. Novikov et al., Phys.Lett. **B240** (1990) 227

2.4.10 Accelerator mass spectrometry with stable ions

Ch. Faude, E. Nolte, S. Xu

For performing ams with stable ions with high sensitivity of the order of 10^{-12} for the concentration of the element Z to be detected in the matrix or crystal of the element Z', the injector has to be constructed as ultra clean facility. The facility under construction at the Munich accelerator laboratory is shown in Fig. 1. The sputtering beam is generated via an oven and an ionizer, analyzed magnetically in a 120° magnet and focussed to the sputter target in the ultra clean sputter chamber (Fig. 2). This part of the beam line in more detail is : ionizer - steerer-einzel lens - focus - 120° magnet - focus - steerer-einzel lens - sputter target. The sputter chamber has slits and electrodes made of ultra clean materials and is pumped efficiently. The sputtered ions are extracted, analyzed by a 90° magnet and sent to the tandem. This part of the beam line in more detail is : sputter target - extraction - quadrupole lens/steerer - einzel lens - 90° magnet - quadrupole lens - focus. The sputtered ions shall be detected at the high energy side of the tandem by an energy loss/ residual energy detector eventually combined with a time-of-flight line.

Applications of this facility are material analysis of ultra clean semiconductor crystals, identification of disturbing long-lived radioactivities in large, very sensitive low-level detectors and detection of double-beta decay products in radiochemical experiments.

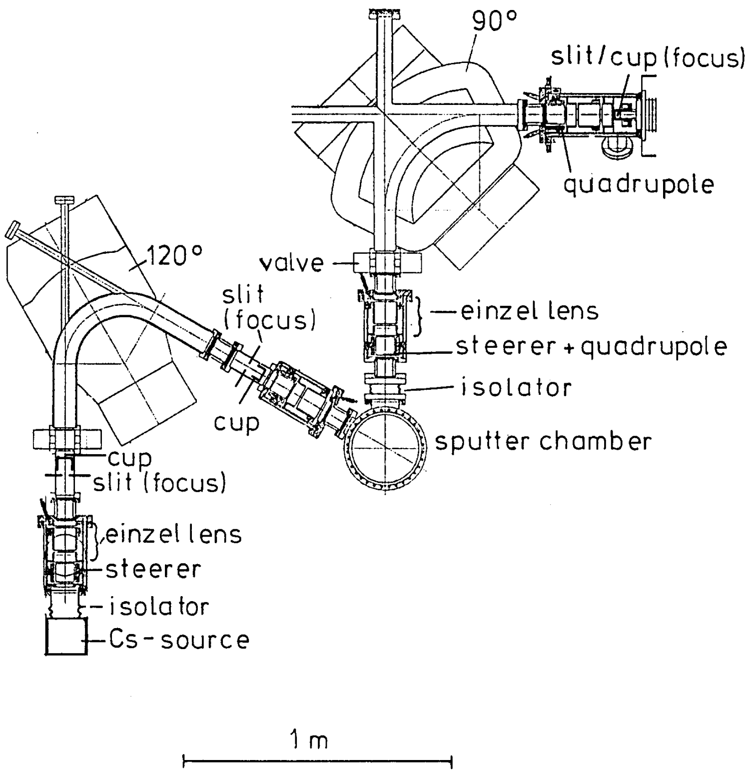

Fig. 1: Beam line system of the injector for ams with stable isotopes

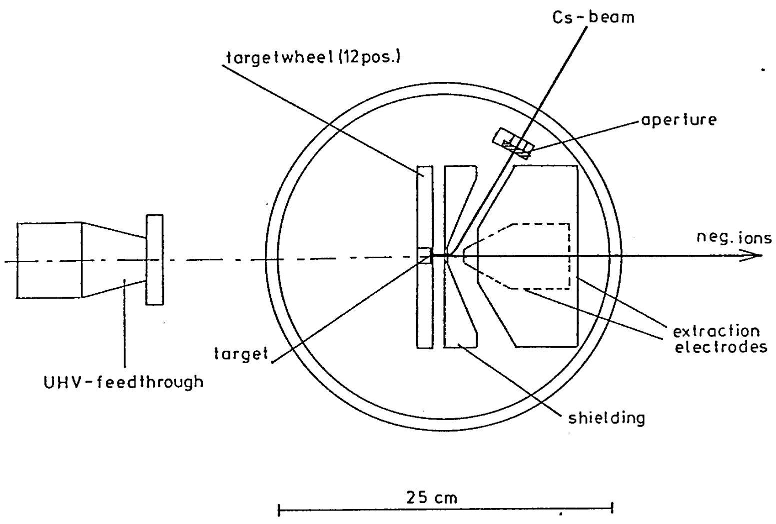

Fig. 2: Sputtering chamber for ams with stable isotopes